CHAPTER 3

MONITORING, CONTROL, AND PROTECTION OF RADIAL DISTRIBUTION NETWORKS THROUGH SMART METERING

3.1 INTRODUCTION

Automation of the distribution system may be an essential requirement in a smart grid architecture. The past work done in this area has certain limitations like not considering the case of load shedding/load reconnection based on the availability of power. Distribution networks are prone to several challenges such as overcurrent through feeder resulting in overheating of conductors, unbalancing of loads on three phases, power thefts due to illegal connections. Reduction of available power at the substation due to under voltage requires some of the loads to be switched OFF to protect various equipments against under voltages. Similarly, increase of available power caused by over voltage requires switching ON of some new loads to protect equipments against over voltages. Handling all such problems through manual switching are time consuming and prone to mistakes thus causing aggravation of situation. Therefore, complete automation of distribution network is the need of the hour where such problems may be automatically detected and controlled. Consumer premises may be provided with smart meters which are capable to interface with controllers at the substation and distribution transformer (DT), through fast bidirectional communication link either wired or wireless. Controllers at the substation and distribution transformers (DTs) having application softwares dealing with distribution network challenges such as overcurrent monitoring and control, load balancing, power theft detection may generate control decisions based on received informations, and automatic implementation of control measures may be processed, accordingly. Most of the challenges

may be handled by local controller at distribution transformers, whereas, remaining may be tackled by master controller at the main substation. Thus, distribution networks may be saved against outages/deterioration of power quality caused due to such problems.

In this Chapter, a smart distribution system has been proposed, where smart meters with communication capabilities play a vital role in the operation of the system. Two-level control architecture has been considered in this work. Primary controller (local controller) installed at distribution transformer generates suitable control strategies to deal with distribution network challenges such as load shedding/load reconnection based on available power at the substation, load balancing, protection of feeder against overcurrent and detection of power theft. Secondary controller (master controller) installed at distribution substation continuously checks available power and instructs primary controllers for load shedding/load reconnection based on the total connected load on the feeder. Two-level control architecture has been developed using MATLAB/SIMULINK for a distribution network consisting of two identical areas, each comprising of 21 loads fed through the three-phase radial feeder. Each radial feeder is supplied from the main substation through the distribution transformer. Simulation results obtained on MATLAB/ SIMULINK model have been validated on an eMEGASim® OP5600 OPAL-RT real-time simulator.

3.2 PROPOSED SMART DISTRIBUTION SYSTEM

In the proposed smart distribution system (shown in Fig. 3.1), primary controllers (local controllers) are placed at all the Distribution Transformers (DTs), whereas, the secondary controller (master controller) is situated at the main substation receiving supply from the grid through the incoming feeder. The master controller is linked to n number of local controllers placed at respective DTs. Local controller 1 set at the first distribution transformer (DT_1) is connected to 'p' number of loads fed by DT_1. Local controller 2 placed

at the second distribution transformer (DT_2) is linked to 'q' number of loads supplied by DT_2. Local controller n placed at nth distribution transformer (DT_n) is linked to the 'r' number of loads fed by DT_n.

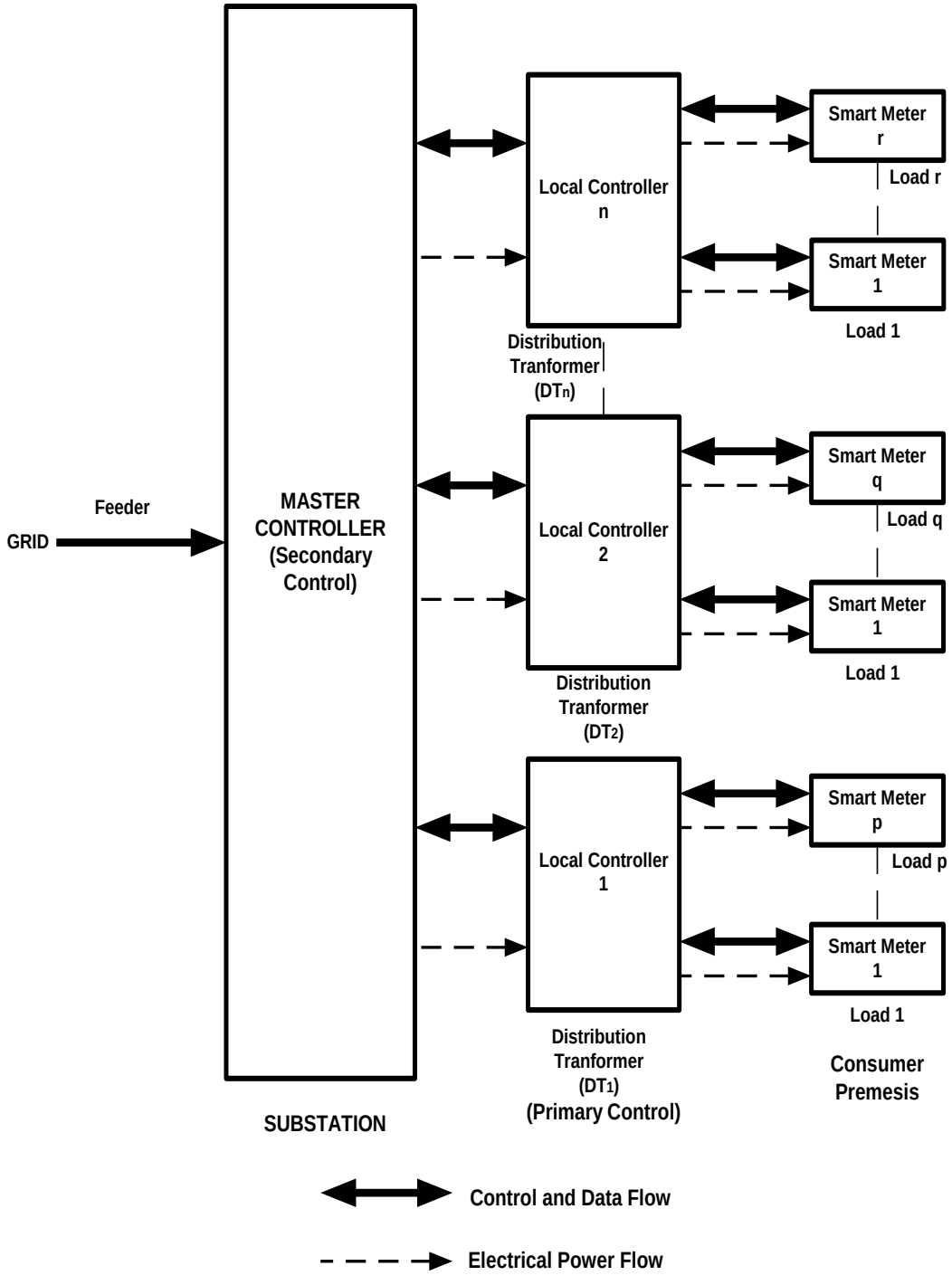

Fig. 3.1 The layout of the proposed smart distribution system

Each load is connected to a smart meter for measurement of various electrical quantities such as voltage, current, real and reactive power consumption, and power factor. Smart meters can also be interfaced/interact with local controllers (which are installed at DTs) through Information and Communication Technology (ICT), which provides the path for the bidirectional flow of information (data and control signals) between the smart meter and local controller. All local controllers installed at DTs are interfaced/linked to the master controller installed at substation via communication links which provide the path for the bidirectional flow of information between the master controller and local controllers.

The master controller compares available power received from the feeder with the total connected load on the substation (data collected from local controllers through smart meters) and instructs local controllers installed at DTs to disconnect/ reconnect loads based on available power at the substation.

Total available power at the substation is distributed proportionately to all DTs based on the total connected load on each distribution transformer on its three phases as per following:

$$P_i = \left(\frac{Pic}{\sum_{i=1}^{n} Pic}\right) P_{available} \quad (3.1)$$

where, P_i = Load shared per phase by i^{th} distribution transformer DT_i;

P_{ic}= Total connected load per phase on DT_i;

n= Total number of distribution transformer in the system;

$P_{available}$= Total available power per phase at the substation.

Available power in a phase ($P_{available}$) at the substation may be given by:

$$P_{available} = V_{ph}\, I_{ph} \cos\emptyset \quad (3.2)$$

where, V_{ph} = Magnitude of phase voltage available at the substation transformer secondary winding (winding on load side);

I_{ph} = Magnitude of the phase current of the substation transformer secondary winding;

cosØ = Power factor of the phase at the substation transformer secondary winding.

It is apparent from (3.2) that the reduction of supply voltage/power factor at the substation causes loss of available power, thus requiring load shedding to be performed. In the absence of load shedding, constant power loads will draw overcurrent, whereas, constant impedance and constant current loads will get reduced supply. To avoid this, loads have been disconnected once available power in a phase differs from the total connected load on that phase by 10% or more. Loads have been reconnected once this difference becomes less than 10%.

Based on information received from the master controller regarding available power, local controllers perform the task of load shedding/load reconnection with due consideration of priority of loads, as per the following algorithm:

1. If available power in phase A is less than the total connected load on phase A by 10%, go to step 2, else go to step 5.
2. Find and shut down the load on phase A, which is approximately equal to the difference between total load (in kW) connected on phase A and available power in phase A (in kW). If found, go to step 3, else go to step 4.
3. Check the priority of that load. If the priority of the load is least, disconnect it immediately, and go to step 1. If the load has a medium priority, wait for a few seconds, if available power becomes normal, go to step 1, else disconnect it and go to step 1. If the load has top priority, don't disconnect it and go to the next step.
4. Search for the next higher load on phase A, and go to step 3.
5. Repeat all steps 1 to 4 for phase B and phase C, respectively.
6. Repeat steps 1 to 5 every one minute.

3.2.1 Functional algorithm for load balancing

The local controller checks the total load on each phase and generates the control signal to balance loads in case of unbalancing above 10%. The functional algorithm for load balancing is presented below:

1. Calculate phase current unbalance (PCU) using:

$$PCU = \frac{|Iph\ A - Iph\ B| + |Iph\ B - Iph\ C| + |Iph\ C - Iph\ A|}{3} \quad (3.3)$$

where, I_{phA}, I_{phB}, and I_{phC} represents distribution transformer secondary winding current magnitude in phase A, phase B, and phase C, respectively.

2. Calculate average phase current magnitude ($I_{ph,average}$) of distribution transformer secondary winding using:

$$I_{ph,average} = \frac{Iph\ A + Iph\ B + Iph\ C}{3} \quad (3.4)$$

3. Calculate phase unbalance factor (PUF) using:

$$PUF = \frac{PCU}{Iph,average} \quad (3.5)$$

4. If PUF is greater than 10%, go to next step, else stop.

5. Calculate average connected real power load (AP_p) and average connected reactive power load (AP_q) of three phases as per the following:

$$AP_p = \frac{Pph\ A + Pph\ B + Pph\ C}{3} \quad (3.6)$$

$$AP_q = \frac{Qph\ A + Qph\ B + Qph\ C}{3} \quad (3.7)$$

where, P_{phA}, P_{phB}, and P_{phC} are the totals connected real power load on phase A, phase B, and phase C, respectively, and Q_{phA}, Q_{phB} and Q_{phC} are the totals connected reactive power load on phase A, phase B, and phase C, respectively.

6. Calculate extra real power load on each phase causing load unbalancing using:

$$P_{A,extra} = P_{phA} - AP_p \quad (3.8)$$

$$P_{B,extra} = P_{phB} - AP_p \quad (3.9)$$

P_C,extra= P_{phC}-AP_p (3.10)

where, P_A,extra= extra real power load on phase A, P_B,extra = extra real power load on phase B, and P_C,extra = extra real power load on phase C.

7. Calculate extra reactive power load on each phase causing load unbalancing using:

Q_A,extra= Q_{phA}-AP_q (3.11)

Q_B,extra= Q_{phB}-AP_q (3.12)

Q_C,extra= Q_{phC}-AP_q (3.13)

where, Q_A,extra= extra reactive power load on phase A, Q_B,extra = extra reactive power load on phase B, and Q_C,extra = extra reactive power load on phase C.

8. Shift lowest connected real power load of phase having the highest extra real power load to a phase having the lowest extra real power load.
9. Shift lowest connected reactive power load of phase having the highest extra reactive power load to phase having the lowest extra reactive power load, and again go to step 4, else stop.
10. Repeat steps 1 to 9 every one minute.

3.2.2 Functional algorithm for overcurrent protection of feeder

The local controller compares DT secondary current in each phase with its rated value. If DT secondary current in a phase exceeds its rated value by 10%, it is considered a case of overcurrent on that phase. In case of overcurrent, loads in that phase which draw power more than sanctioned demand and have power factor less than 0.85 lagging, are detected from smart meter readings and are disconnected considering such loads to be a cause of producing overcurrent. However, top priority loads are not disconnected even if they draw more than sanctioned demand and have a power factor less than 0.85 lagging. Disconnected loads are reconnected once, DT secondary current in that phase becomes less than 1.1 times

its rated value. Functional algorithm for overcurrent protection of feeder is presented below:

1. If DT secondary current in Phase A ($I_{s,\ A}$) is greater than rated DT secondary current ($I_{s,\ rated}$) by 10%, go to step 2, else, go to step 4.
2. Check all smart meter readings of phase A. Disconnect loads in phase A, drawing more than sanctioned demand and having power factor less than 0.85 lagging without disturbing top priority loads, and go to the next step.
3. Recheck DT secondary current in Phase A. If DT secondary current in phase A differs from its rated value by less than 10%, reconnect disconnected loads and go to step 4, else, go to step 2.
4. If DT secondary current in Phase B ($I_{s,\ B}$) is greater than rated DT secondary current ($I_{s,\ rated}$) by 10%, go to step 5, else, go to step 7.
5. Check all smart meter readings of phase B. Disconnect loads in phase B drawing more than sanctioned demand and having power factor less than 0.85 lagging without disturbing top priority loads, and go to the next step.
6. Recheck DT secondary current in Phase B. If DT secondary current in phase B differs from its rated value by less than 10%, reconnect disconnected loads and go to step 7, else, go to step 5.
7. If DT secondary current in Phase C ($I_{s,\ C}$) is greater than rated DT secondary current ($I_{s,\ rated}$) by 10%, go to step 8, else, stop.
8. Check all smart meter readings of phase C. Disconnect loads in phase C, drawing more than sanctioned demand and having power factor less than 0.85 lagging without disturbing top priority loads, and go to the next step.

9. Recheck DT secondary current in Phase C. If DT secondary current in phase C differs from its rated value by less than 10%, reconnect disconnected loads, and stop else, go to step 8.
10. Repeat steps 1 to 9 every one minute.

3.2.3 Functional algorithm for theft detection

The local controller compares the magnitude of current in each phase of the secondary winding of DT with the magnitude of the vector sum of currents drawn by connected loads on that phase. An illegal connection in a phase is bound to produce the difference between the magnitude of DT secondary current and magnitude of the vector sum of load currents on that phase. However, a small difference may occur due to the error in meter readings. Therefore, the difference of 10% or more between the magnitude of DT secondary current in a phase and magnitude of phasor sum of currents drawn by different legal loads on that phase has been considered as power theft on that phase, in this work. The complex current drawn by each load is calculated using current and power factor readings of smart meters along with complex voltage drop calculated for different sections of the feeder concerning a common reference. Functional algorithm for detection of power theft is presented below:

1. Calculate $[I_{s,\,A} - |\sum \bar{I}_{ph,\,A}|] \,/\, [|\sum \bar{I}_{ph,\,A}|]$

   where, $I_{s,\,A}$ = Magnitude of current in phase A of DT secondary winding;

   $|\sum \bar{I}_{ph,\,A}|$ = Magnitude of phasor sum of complex current drawn by each legal load connected to phase A;

   If $[I_{s,\,A} - |\sum \bar{I}_{ph,\,A}|] \,/\, [|\sum \bar{I}_{ph,\,A}|]$ is greater than 10%, notify theft in phase A, else, go to next step.

2. Calculate $[I_{s,\,B} - |\sum \bar{I}_{ph,\,B}|] \,/\, [|\sum \bar{I}_{ph,\,B}|]$

   where, $I_{s,\,B}$ = Magnitude of current in phase B of DT secondary winding;

   $|\sum \bar{I}_{ph,\,B}|$ = Magnitude of phasor sum of complex current drawn by each legal load connected to phase B;

If $[I_{s,B} - |\sum \bar{I}_{ph,B}|] / [|\sum \bar{I}_{ph,B}|]$ is greater than 10%, notify theft in phase B, else, go to next step.

3. Calculate $[I_{s,C} - |\sum \bar{I}_{ph,C}|] / [|\sum \bar{I}_{ph,C}|]$

   where, $I_{s,C}$ = Magnitude of current in phase C of DT secondary winding;

   $|\sum \bar{I}_{ph,C}|$ = Magnitude of phasor sum of complex current drawn by each legal load connected to phase C;

   If $[I_{s,C} - |\sum \bar{I}_{ph,C}|] / [|\sum \bar{I}_{ph,C}|]$ is greater than 10%, notify theft in phase C, and stop.

4. Repeat steps 1 to 3 every one minute.

3.2.4 Simultaneous control of events: load balancing, overcurrent protection of feeder, and power theft

The flowchart for simultaneous control of load balancing, overcurrent protection of feeder, and power theft detection and elimination has been shown in Fig. 3.2. As per this flowchart, master controller checks the available power at the substation and decides load sharing of each DT as per equation (3.1), and disconnects/connects loads on three phases of the feeder as per algorithm presented in Section 3.2. The local controller present at DTs, checks the total load on each phase based on informations received from smart meters placed at consumer premises, and generates the control signal to balance loads as per algorithm 3.2.1 in case of unbalancing above 10%. Once, loads on three phases get balanced, local controller present at DTs checks secondary current in each phase of DT. If DT secondary current in any of the phase exceeds its rated value by 10%, it is considered a case of overcurrent on that phase. An overcurrent in a phase may be caused either by switching ON of excess legal loads or it may be as a result of power theft due to switching of illegal connections. In order to detect power theft, first theft detection algorithm is run as per Section 3.2.3. If theft is detected, an alarm is generated for the operators to disconnect the illegal loads. However, if no theft is detected then algorithm for overcurrent protection of the feeder is run as per Section 3.2.2. Since, algorithm for

overcurrent protection of feeder disconnects some of loads causing overcurrent, it is quite likely that phases become unbalanced. Therefore, percentage unbalance factor (PUF) is checked once again. In case PUF is found to be more than 10%, functional algorithm for load balancing is run again as shown, else available power is rechecked at the substation and all the algorithms are run in coordination as per flowchart shown in Fig. 3.2.

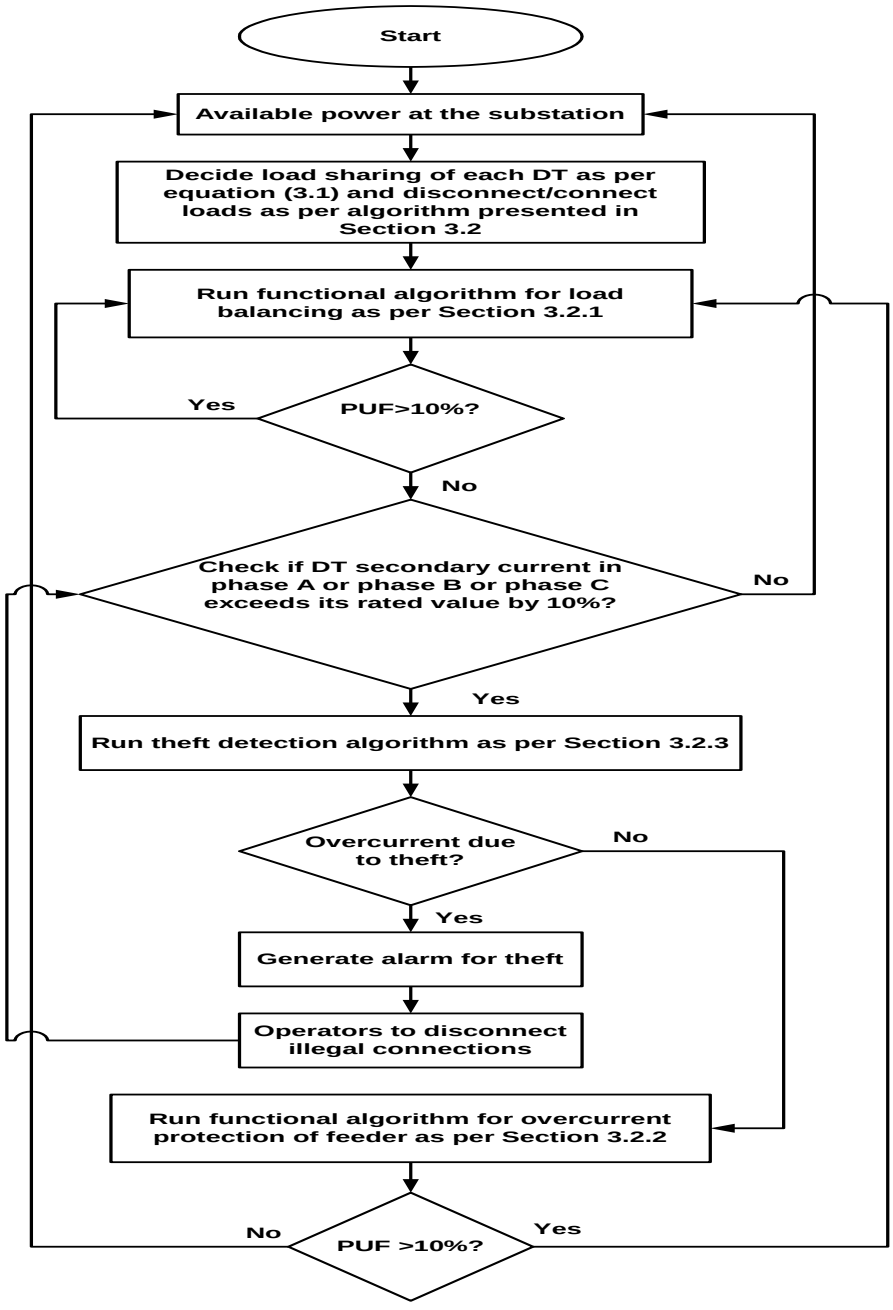

Fig. 3.2 Flowchart for simultaneous control of events: load balancing, overcurrent protection of feeder, and power theft detection and elimination

3.3 CASE STUDIES

Case studies were performed on a smart distribution test system shown in Fig. 3.3. The considered test system consists of two identical areas each comprising of 21 loads fed through the three-phase radial feeder of 3.5km (2.175 miles) length having a series impedance (Z) of (0.1535+j0.3849) ohms/mile [48]. Each area contains the combination of top priority, medium priority, and least priority loads. Load details of an area for phase A, phase B, and phase C have been shown in Table 3.1, Table 3.2, and Table 3.3, respectively. Total connected real power demand and reactive power demand in an area are 2145kW and 945kVAr, respectively, with the real and reactive power demand of 715kW and 315kVAr, respectively, on each phase. Total sanctioned real and reactive power demand in an area are 2265kW and 1050kVAr, respectively, with the real and reactive power demand of 755kW and 350kVAr, respectively, on each phase. Each load is placed with a smart meter. Two areas are fed through distribution transformers DT_1 and DT_2, respectively, each rated 2.5MVA, 50Hz, 6.6kV/415V. Distribution transformers are supplied from 33kV distribution substation through substation transformer rated 5MVA, 50Hz, 33kV/6.6kV. The 33kV distribution substation gets power injected to it from the grid through the 33kV incoming feeder.

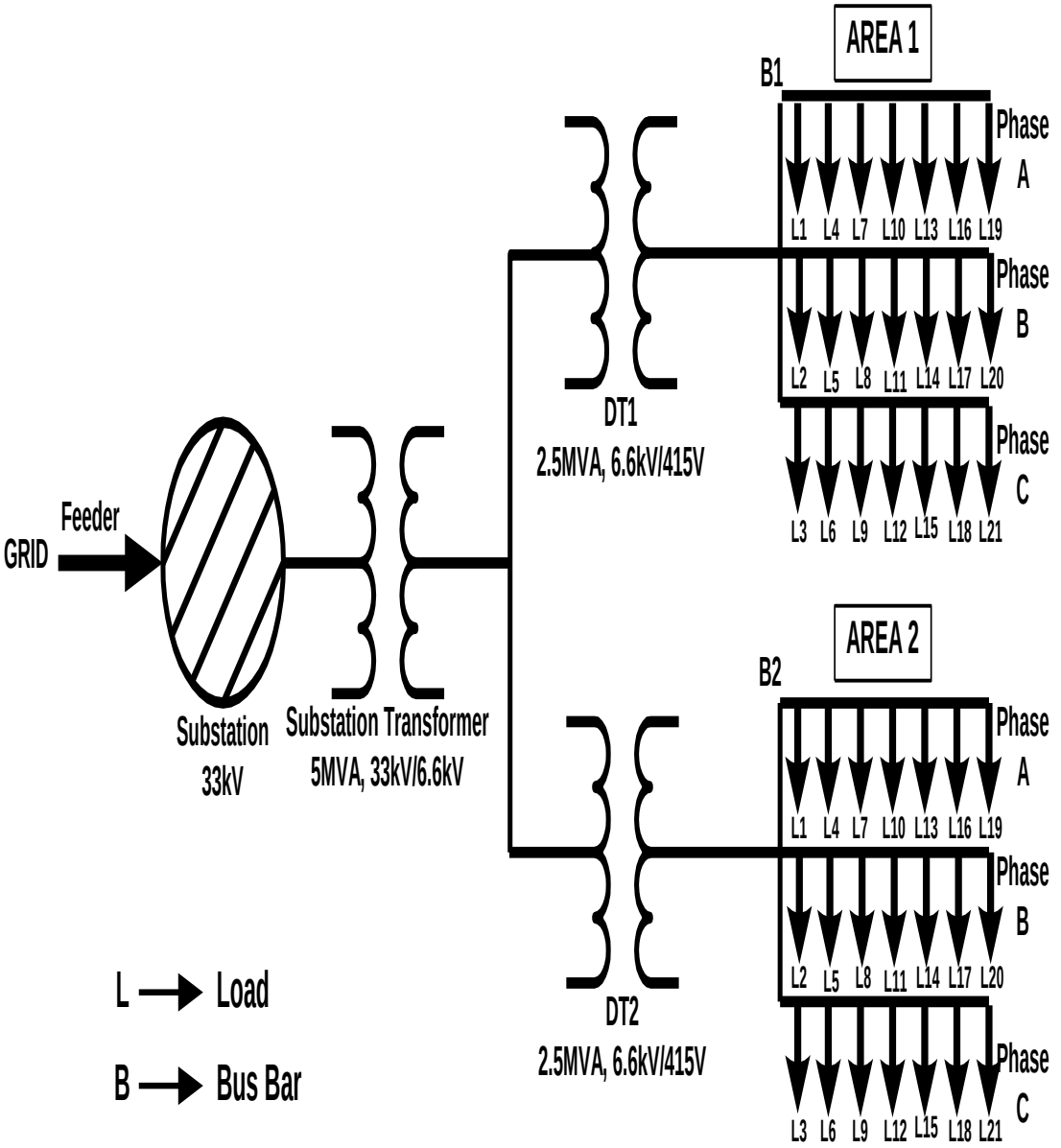

Fig. 3.3 Single line diagram of the smart distribution test system

TABLE 3.1 LOAD DETAILS OF AREA 1/AREA 2 FOR PHASE A

Load on phase A					
Load Number	Connected Load		Sanctioned Load		Load Priority*
	kW	kVAr	kW	kVAr	
1	105	45	110	50	2
4	90	25	105	30	2
7	95	55	100	60	1
10	120	55	130	60	3
13	110	50	110	55	3
16	100	35	100	40	3
19	95	50	100	55	3
Total	715	315	755	350	

*1- Top priority, 2- Medium priority, 3- Least priority

TABLE 3.2 LOAD DETAILS OF AREA 1/AREA 2 FOR PHASE B

Load on phase B					
Load Number	Connected Load		Sanctioned Load		Load Priority*
	kW	kVAr	kW	kVAr	
2	125	60	135	65	1

5	100	50	105	55	2
8	120	65	125	70	3
11	85	35	95	40	2
14	90	35	90	40	3
17	80	35	90	40	3
20	115	35	115	40	3
Total	715	315	755	350	

*1- Top priority, 2- Medium priority, 3- Least priority

TABLE 3.3 LOAD DETAILS OF AREA 1/AREA 2 FOR PHASE C

Load on phase C					
Load Number	Connected Load		Sanctioned Load		Load Priority*
	kW	kVAr	kW	kVAr	
3	75	35	75	40	2
6	130	55	140	60	2
9	90	45	95	50	3
12	120	45	135	50	2
15	105	45	105	50	3
18	100	45	105	50	2
21	95	45	100	50	2
Total	715	315	755	350	

*1- Top priority, 2- Medium priority, 3- Least priority

Algorithms presented in Section 3.2 regarding load shedding/load reconnection based on available power, load balancing, overcurrent protection of feeder and theft detection were tested on a developed MATLAB /SIMULINK model of the test system as well as on an eMEGASim® OP5600 OPAL-RT real-time simulator. Simulation results are presented below:

3.3.1 Load shedding/Load reconnection based on available power

The master controller continuously checked total available power at the substation in every one minute and decided the distribution of available power to distribution transformers DT_1 and DT_2 connected to two areas based on the total connected load in each area. The plot of available power of phase A in area 1 versus (vs.) time and the total connected load of phase A in area 1 vs. time have been shown in Fig. 3.4 for simulation done on MATLAB/ SIMULINK model. It is observed from Fig. 3.4 that available power drops from 709kW to 590kW at time t=0.56sec, whereas, total connected load at this instant is 665kW. Since available power is less than total connected load by 11.3%, master controller present at substation instructs local controller at DT_1 to perform load shedding as per algorithm presented in Section 3.2, and loads are disconnected as shown. It is observed from Fig. 3.4 that available power is recovered to 709kW at time t=0.75sec; therefore, loads are reconnected as shown. Breaker status of load 7 (a top priority load) has been shown in Fig. 3.5. It is observed from Fig. 3.5 that the breaker status of load 7 is always ON (status 1) indicating that top priority loads are not disturbed while performing load shedding.

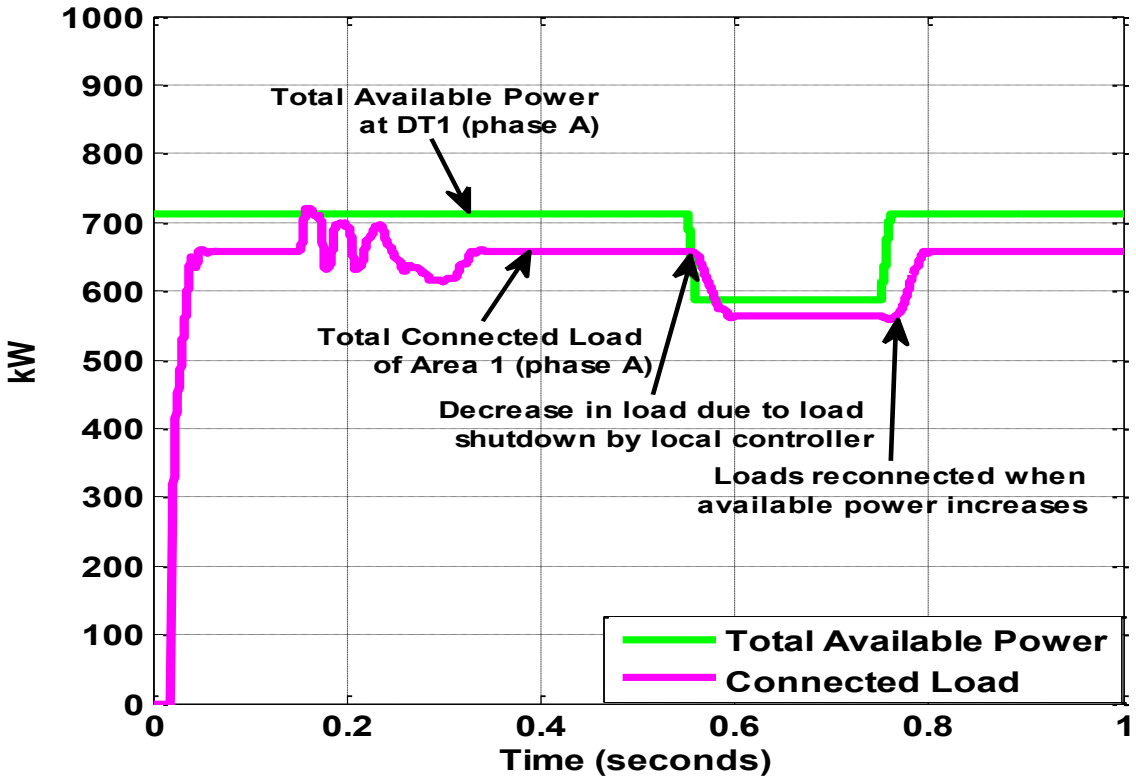

Fig. 3.4 Total available real power and the total connected load of phase A in area1

(MATLAB/SIMULINK results)

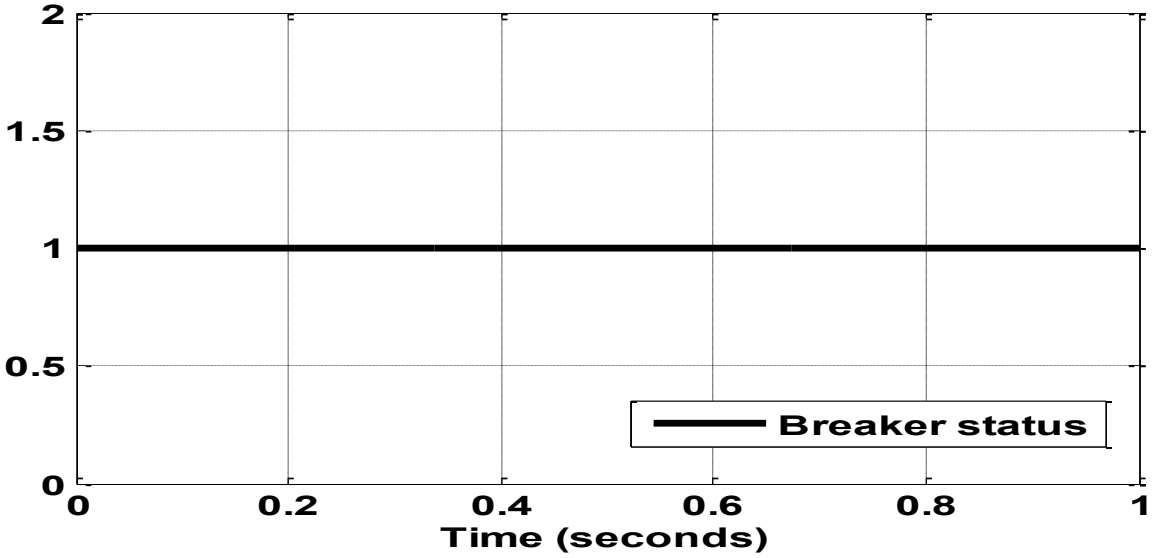

Fig. 3.5 Breaker status of load 7 having top priority

(MATLAB/SIMULINK results)

The plot of available power of phase A in area 1 vs. time and the total connected load of phase A in area 1 vs. time were also obtained on eMEGASim® OP5600 OPAL-RT real-

time simulator. The plots have been shown in Fig. 3.6. It is observed from Fig. 3.6 that available power drops from 709kW to 580kW at time t=0.56sec, whereas, total connected load at this instant is 665kW. Since available power is less than total connected load by 12.8%, master controller present at substation instructs local controller at DT_1 to perform load shedding as per algorithm presented in Section 3.2, and loads are disconnected as shown. It is observed from Fig. 3.6 that available power is recovered to 709kW at time t=0.75sec; therefore, loads are reconnected as shown. Breaker status of top priority load number 7 obtained on OPAL-RT real-time simulator has been shown in Fig. 3.7. It is observed from Fig. 3.7 that the breaker status of load 7 is always ON (status 1) indicating that top priority loads are not disturbed while performing load shedding.

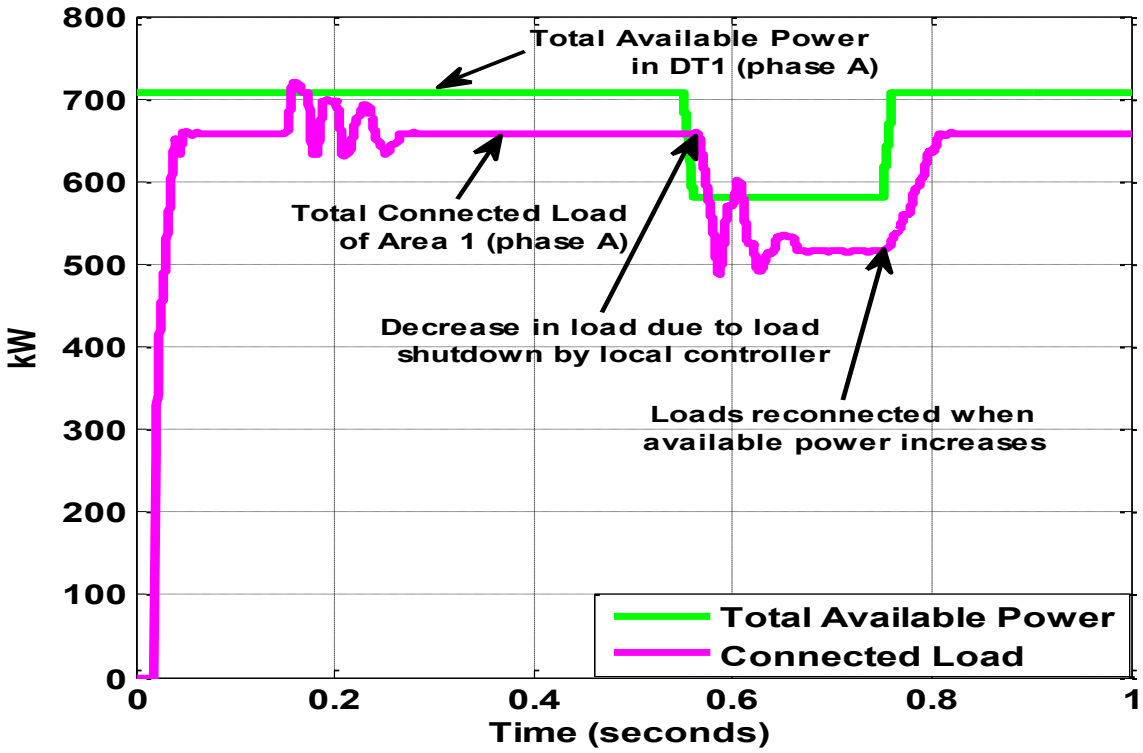

Fig. 3.6 Total available real power and the total connected load of phase A in area1

(OPAL-RT real-time simulator results)

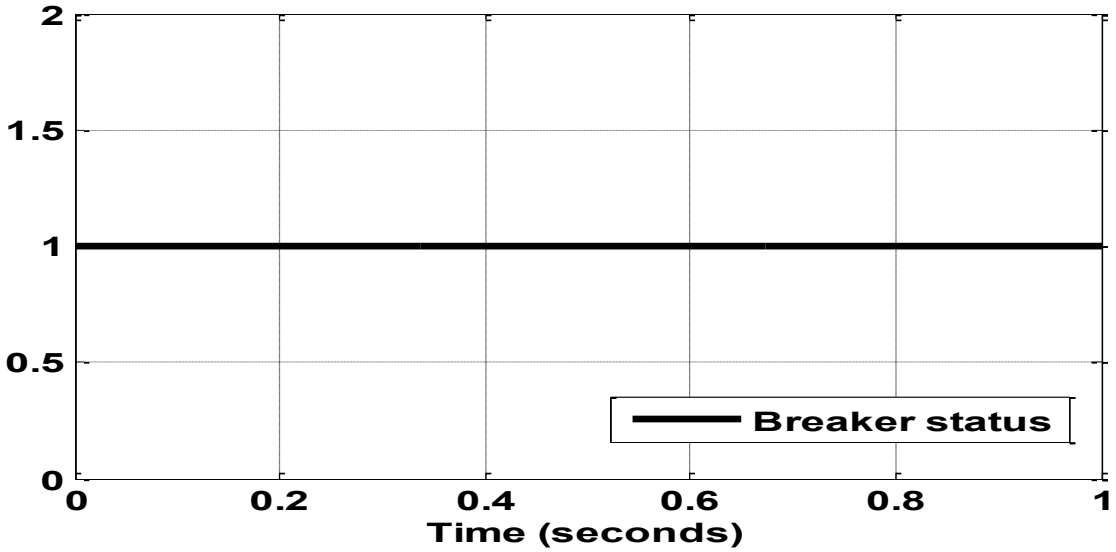

Fig. 3.7 Breaker status of load 7 having top priority

(OPAL-RT real-time simulator results)

It is observed from Fig. 3.4, Fig. 3.5, Fig. 3.6 and Fig. 3.7 that simulation results on eMEGASim® OP5600 OPAL-RT real-time simulator closely match with results obtained on the MATLAB/ SIMULINK model of the test system.

3.3.2 Load balancing

MATLAB/SIMULINK results of load balancing process of area 2 by the local controller are presented below:

The plot of DT_2 secondary phase currents (root mean square (RMS) value) vs. time has been shown in Fig. 3.8, whereas, the plot of percentage phase unbalance factor (PUF) vs. time has been shown in Fig. 3.9. It is observed from Fig. 3.9 that PUF was less than 10% up to 0.16sec, thus requiring no action regarding load balancing. Load number 8 and load number 20 of phase B were switched off at time t=0.16sec. This caused the drop in phase B current to a value of 2030A, whereas, phase A and phase C currents remain intact as shown in Fig. 3.8. This resulted in PUF (computed from equations (3.3) to (3.5)) of 18.7% which is more than 10% as shown in Fig. 3.9. Therefore, extra real and reactive power demands of each of the phases were calculated as per equations (3.6) to (3.13).

It resulted in extra real power demand of 70.77kW, -140.66kW, and 70kW for phase A, phase B and phase C respectively, whereas, extra reactive power demand of 34.68kVAr, -68.67kVAr, and 34kVAr for phase A, phase B and phase C, respectively. As Phase A was having highest extra real as well as reactive power demand, whereas, phase B was having lowest extra real and reactive power demand, lowest connected load on phase A (load number 4 that was drawing lowest real and reactive power demand of 77.32kW and 37.77kVAr, respectively at that instant) was shifted to phase B at time t=0.25sec as shown in Fig. 3.8. This brought down the PUF to less than 10% value at time t=0.36sec, as observed from Fig. 3.9. Therefore, load number 8 and load number 20 were reconnected at time t=0.36sec, as shown in Fig. 3.8. Reconnection of load number 8 and load number 20 of phase B caused the rise in phase B current to 3320A (as observed from Fig. 3.8) which resulted in PUF of 15.24% which was more than 10% again, as observed from Fig. 3.9. PUF was computed using equations (3.3) to (3.5). Extra real and reactive power demand were computed for each of three phases using equations (3.6) to (3.13). It resulted in extra real power demand of -70.37kW, 75.79kW and 74.23kW for phase A, phase B and phase C respectively, whereas extra reactive power demand of -33.52kVAr, 34.26kVAr and 29.63kVAr for phase A, phase B and phase C, respectively. As phase B was having highest extra real power demand as well as reactive power demand, whereas, phase A was having lowest extra real and reactive power demand, lowest connected load on phase B (load number 11 that was drawing lowest real and reactive power of 73.93kW and 26.93kVAr, respectively, at that instant) was shifted to phase A at time t=0.41sec as shown in Fig. 3.8. This brought down the phase unbalance factor to less than 10% as observed from Fig. 3.9.

Phase voltages of DT2 secondary winding have been shown in Fig. 3.10. It is observed from Fig. 3.10 that DT2 secondary voltage of three phases fluctuates during load unbalancing. However, once loads on three phases become balanced, three phase voltages gets flattened.

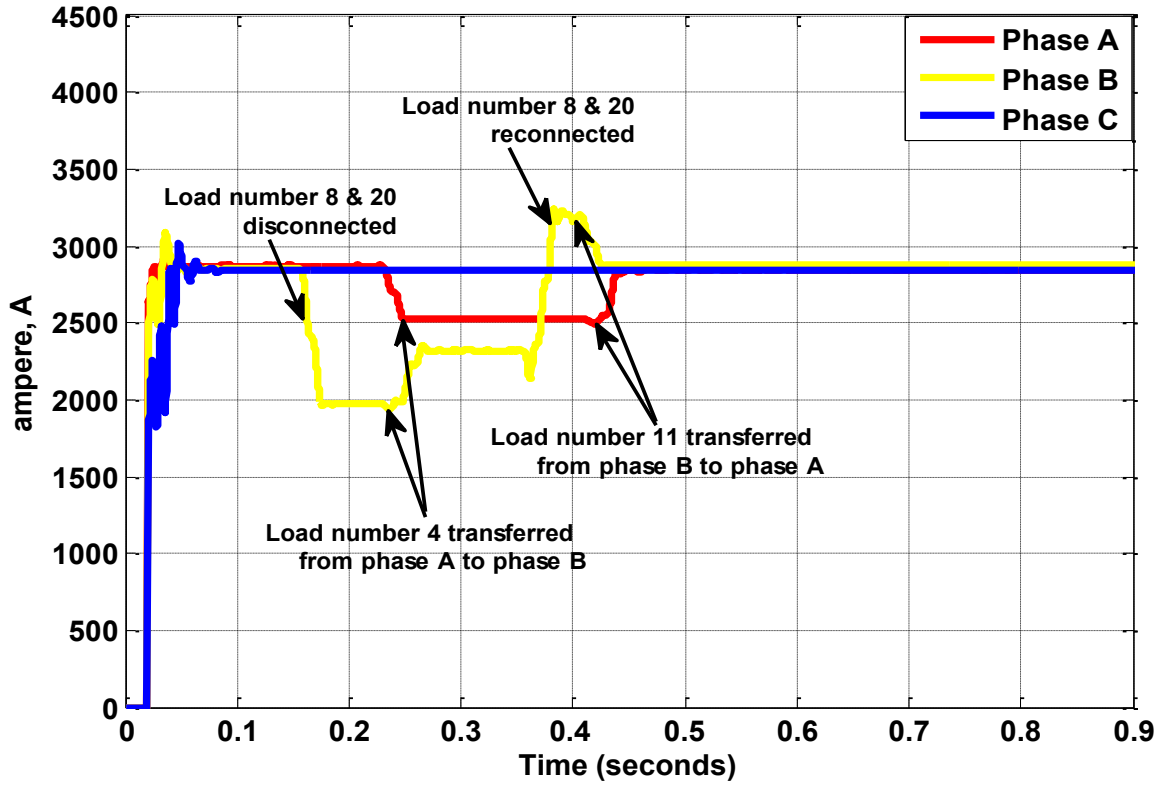

Fig. 3.8 Phase currents (RMS value) of DT_2 secondary winding in case of load balancing process (MATLAB/ SIMULINK results)

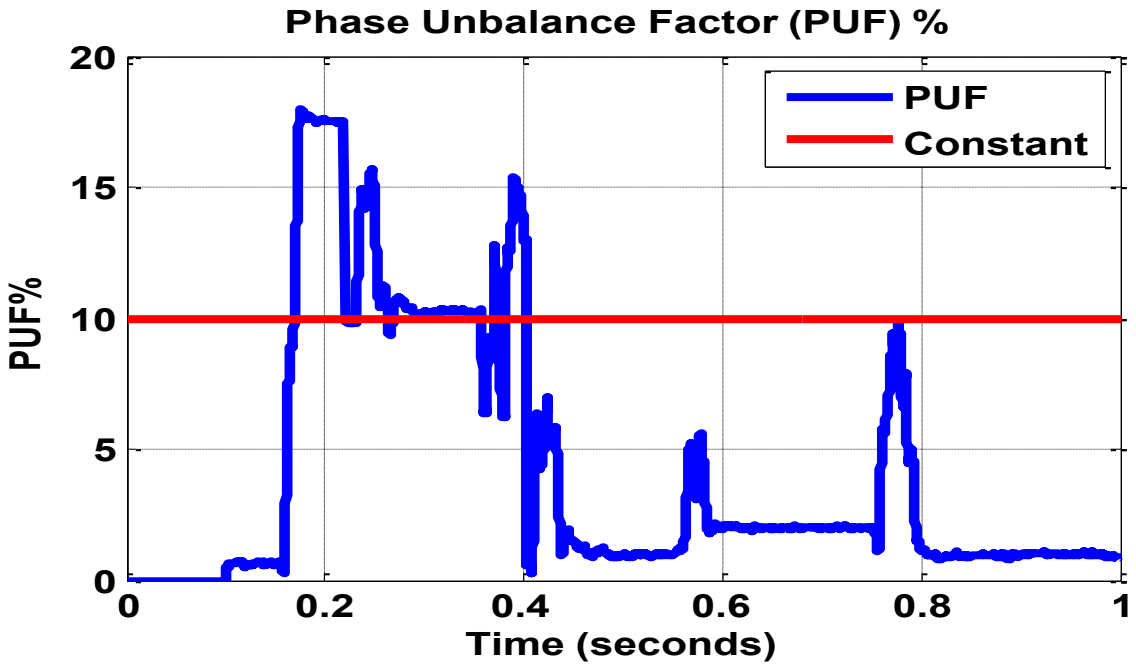

Fig. 3.9 Percentage phase unbalance factor

(MATLAB/ SIMULINK results)

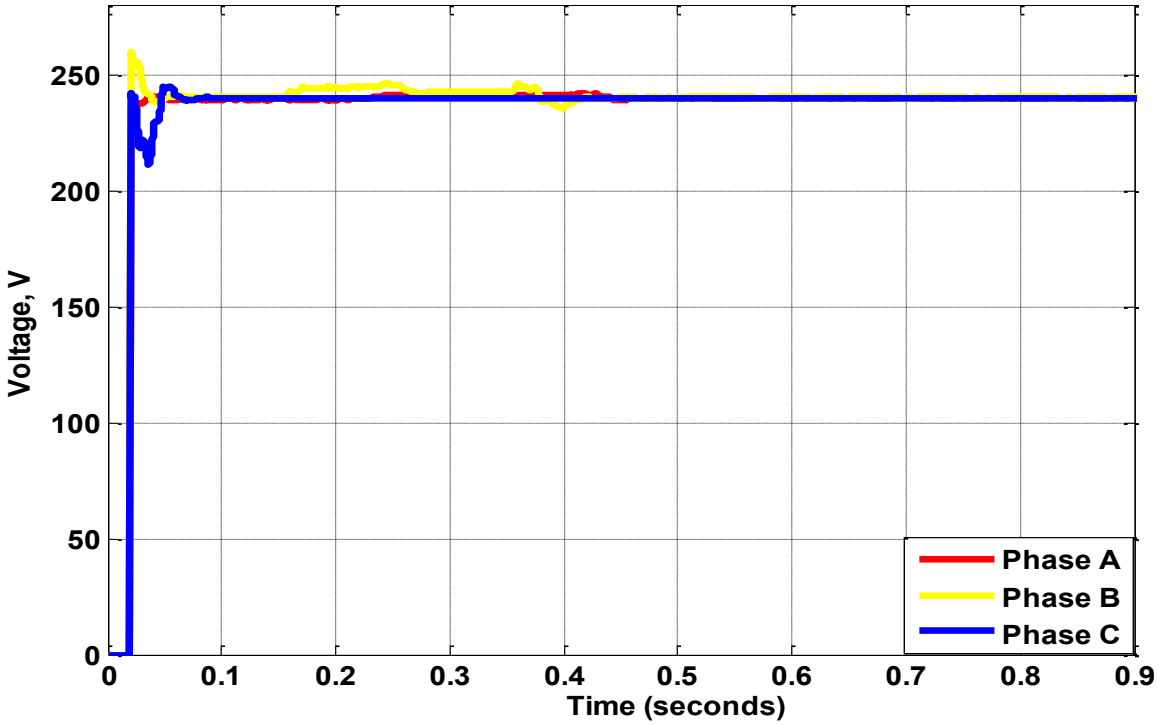

Fig. 3.10 Phase voltages (RMS value) of DT_2 secondary winding in case of load balancing process (MATLAB/ SIMULINK results)

Simulation results of eMEGASim® OP5600 OPAL-RT real-time simulator regarding load balancing by the local controller are presented below:

The plot of DT_2 secondary phase currents (root mean square (RMS) value) vs. time has been shown in Fig. 3.11, whereas, the plot of percentage phase unbalance factor (PUF) vs. time has been shown in Fig. 3.12. It is observed from Fig. 3.12 that PUF was less than 10% up to 0.158sec, thus requiring no action regarding load balancing. Load number 8 and load number 20 of phase B were switched off at time t=0.158sec. This caused the drop in phase B current to a value of 2093.94A, whereas, phase A and phase C currents remain intact as shown in Fig. 3.11. This resulted in PUF (computed from equations (3.3) to (3.5)) of 15.7% which is more than 10% as shown in Fig. 3.12. Therefore, extra real and reactive power demands of each of the phases were calculated as per equations (3.6) to (3.13).

It resulted in extra real power demand of 71kW, -141.76kW, and 70kW for phase A, phase B and phase C respectively, whereas, extra reactive power demand of 35.58kVAr, -69.57kVAr, and 34kVAr for phase A, phase B and phase C, respectively. As Phase A was having highest extra real as well as reactive power demand, whereas, phase B was having lowest extra real and reactive power demand, lowest connected load on phase A (load number 4 that was drawing lowest real and reactive power demand of 77.32kW and 37.77kVAr, respectively at that instant) was shifted to phase B at time t=0.25sec as shown in Fig. 3.11. This brought down the phase unbalance factor to less than 10% value at time t=0.36sec, as observed from Fig. 3.12. Therefore, load number 8 and load number 20 were reconnected at time t=0.36sec, as shown in Fig. 3.11. Reconnection of load number 8 and load number 20 of phase B caused the rise in phase B current to 3290A (as observed from Fig. 3.8) which resulted in phase unbalance factor of 13.2% which was more than 10% again, as observed from Fig. 3.12. PUF was computed using equations (3.3) to (3.5). Extra real and reactive power demand were computed for each of three phases using equations (3.6) to (3.13). It resulted in extra real power demand of -71.37kW, 74.79kW and 73.23kW for phase A, phase B and phase C respectively, whereas extra reactive power demand of -34.52kVAr, 33.26kVAr and 30.63kVAr for phase A, phase B and phase C, respectively. As phase B was having highest extra real power demand as well as reactive power demand, whereas, phase A was having lowest extra real and reactive power demand, lowest connected load on phase B (load number 11 that was drawing lowest real and reactive power of 73.93kW and 26.93kVAr, respectively, at that instant) was shifted to phase A at time t=0.41sec as shown in Fig. 3.11. This brought down the phase unbalance factor to less than 10% as shown in Fig. 3.12.

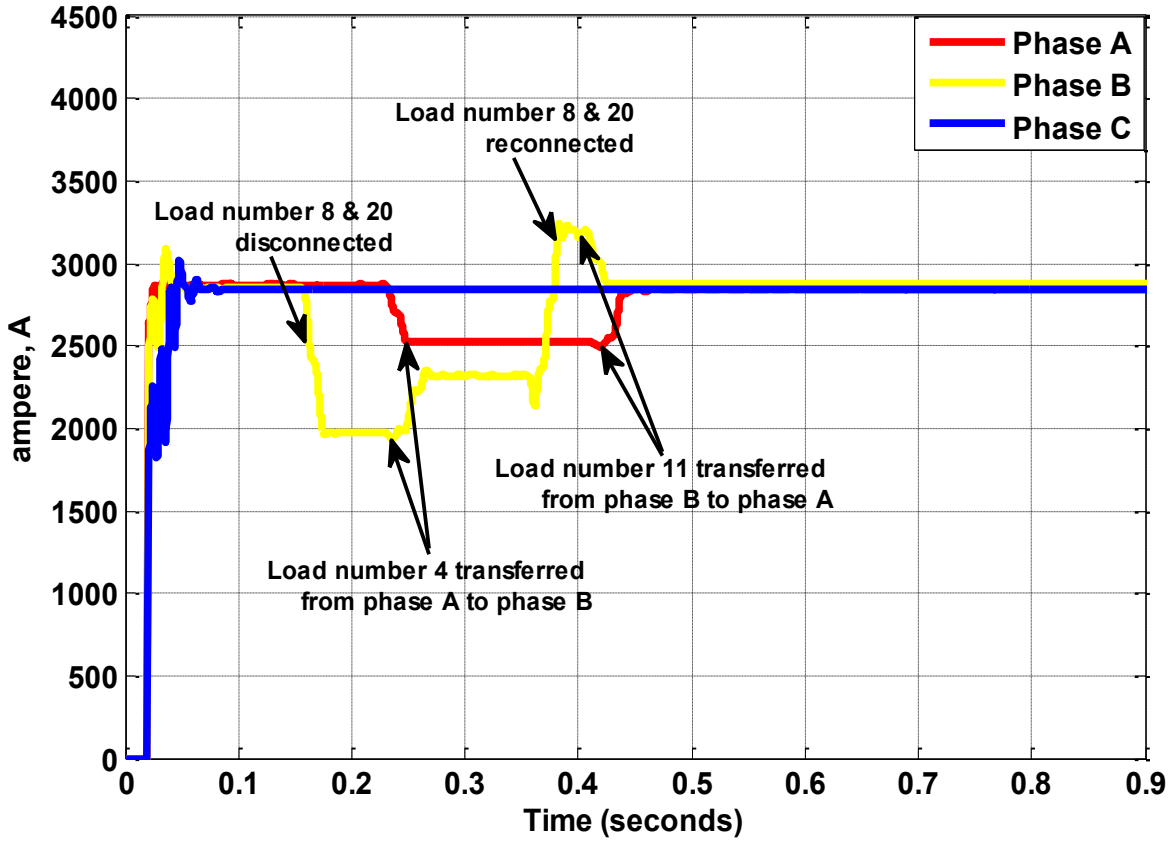

Fig. 3.11 Phase currents (RMS value) of DT_2 secondary winding in case of load balancing process (OPAL-RT results)

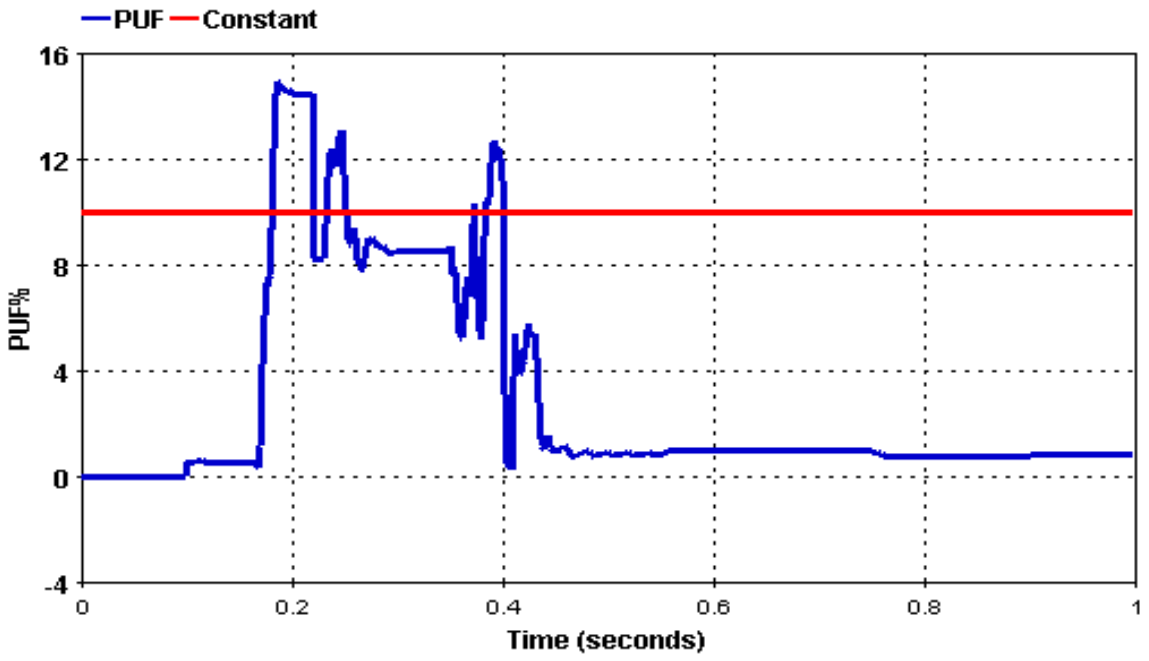

Fig. 3.12 Percentage phase unbalance factor (OPAL-RT results)

It is observed from Fig. 3.8, Fig. 3.9, Fig. 3.11 and Fig. 3.12 that simulation results of load balancing process obtained on MATLAB/SIMULINK model closely match with results obtained on eMEGASim® OP5600 OPAL-RT real-time simulator.

3.3.3 Overcurrent protection of feeder

An extra load consisting of real power demand and reactive power demand of 150kW and 150kVAr, respectively, was connected to load number 1 of phase A in area 1 at time t=0.15sec to produce overcurrent and was removed at time t=0.2sec.

Simulations carried out on MATLAB/SIMULINK model regarding protection against overcurrent of three-phase feeder supplying area 1 by local controller placed at DT_1, are presented below:

The plot of phase currents (RMS value) vs. the time of DT_1 secondary winding has been shown in Fig. 3.13 and the plot of phase voltages (RMS value) vs. time of DT_1 secondary winding have been shown in Fig. 3.14. It is observed from Fig. 3.13 that current in phase A of DT_1 secondary winding exceeded by 15.3% from its rated value of 3478 amperes at time t=0.16sec. Since phase current exceeded by more than 10%, it was considered a case of overcurrent in phase A, by the local controller. Local controller checked smart meter readings of all the loads connected in phase A of area 1. It was observed that load number 1 demand exceeded its sanctioned value and power factor of load number 1 was 0.847, which was slightly less than 0.85. A smart meter reading of all other loads connected to phase A was observed to be less than their sanctioned demand value, and their power factor were also more than 0.85. Therefore, the local controller placed at DT_1 considered power drawn by load number 1 as the cause of overcurrent, and disconnected it at time t=0.17sec, as shown in Fig. 3.13. It is observed from Fig. 3.13 that phase A current of DT_1 secondary winding is brought down to less than 1.1 times of its rated value at time t=0.17sec due to disconnection of load number 1 at time t=0.17sec. Therefore, load number 1 was reconnected at time t=0.18sec. It is observed from Fig. 3.13 that the reconnection of load number 1 again exceeded phase A current by 12% at time t=0.19sec, as the extra load connected to load number 1 again became ON. Sensing overcurrent, local controller checked reading of all smart meters connected to phase A. It was observed that load number 1 was still drawing more than sanctioned demand. Hence, the local controller disconnected it at time t=0.197sec. Disconnection of load number 1 brought down phase A current to less than 1.1 times DT_1 secondary winding rated current value at time t=0.2sec, as observed from Fig. 3.13.

Therefore load number 1 was reconnected by the local controller at time t=0.207sec. It is observed from Fig. 3.14 that overcurrent in phase A causes voltage dip, whereas, voltage rises on load reconnection. Three phase voltages get flattened once feeder overcurrent is eliminated. Breaker status of load number 1 has been shown in Fig. 3.15. It is observed from Fig. 3.15 that breaker status of load number 1 is 0 (i.e., OFF status) for the period 0.17sec to 0.18sec and 0.197sec to 0.207sec, whereas, its status is 1 (i.e., ON status) for the remaining period. This is because load number 1 was disconnected by the local controller at time t=0.17sec, switched ON at time t=0.18sec, again disconnected at time t=0.197sec, and again switched ON at time t=0.207sec.

It is further observed from Fig. 3.13 that phase C current of DT_1 secondary winding exceeded its rated value of 3478 amperes by 19.4% at time t=0.228sec. Local controller checked all smart meter readings connected to phase C. None of the smart meter readings connected to phase C was found to exceed its sanctioned demand value/power factor becoming less than 0.85. Hence, further investigations were carried out regarding power theft in phase C. Simulation results regarding power theft detection have been presented in Section 3.3.4.

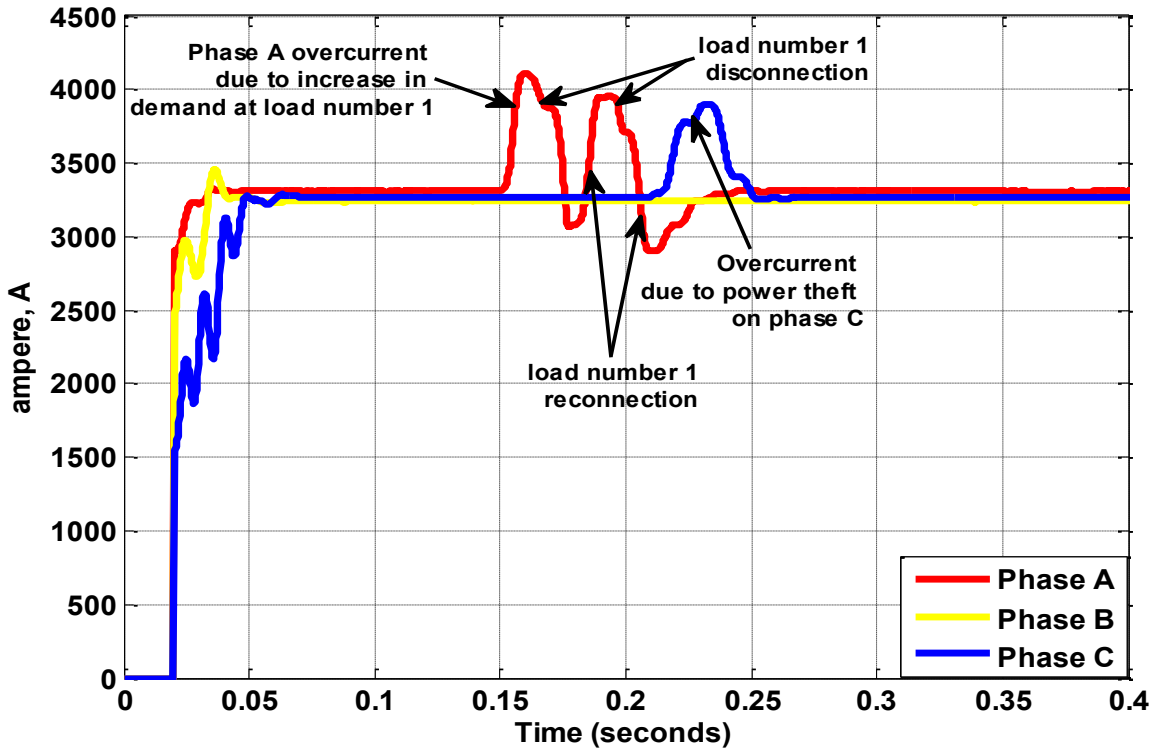

Fig. 3.13 Phase currents (RMS value) of DT_1 secondary winding in case of overcurrent in the feeder (MATLAB/ SIMULINK results)

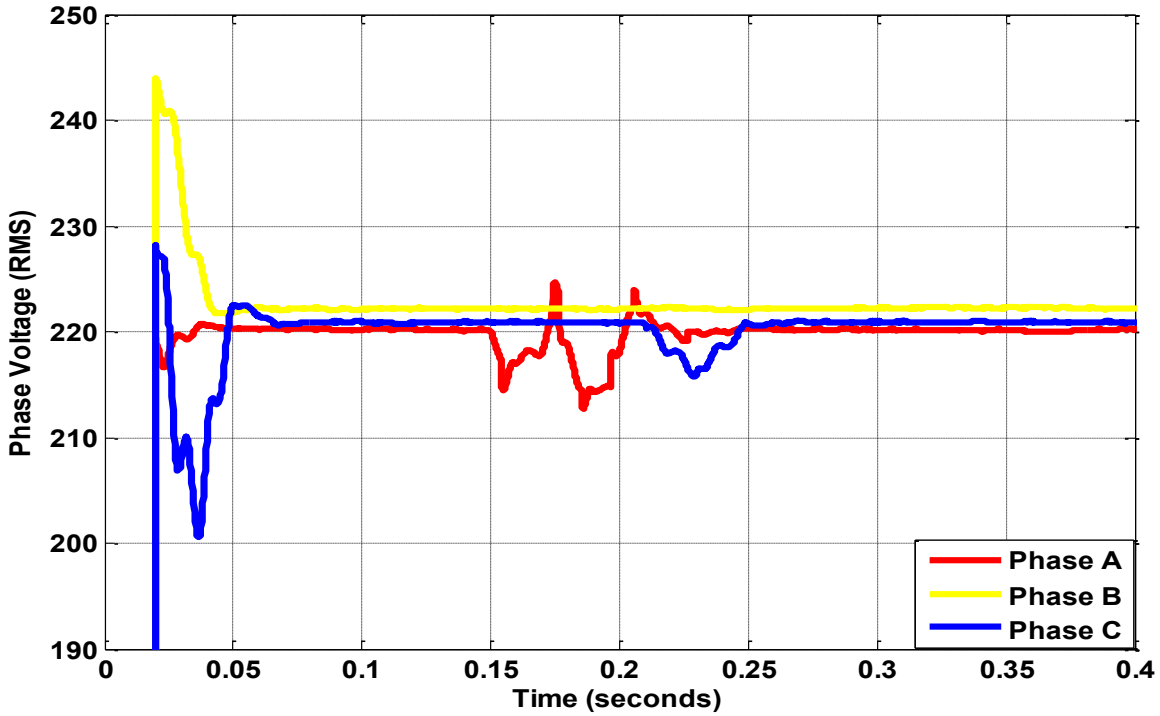

Fig. 3.14 Phase voltages (RMS value) of DT_1 secondary winding (in case of overcurrent and power theft) in the feeder (MATLAB/ SIMULINK results)

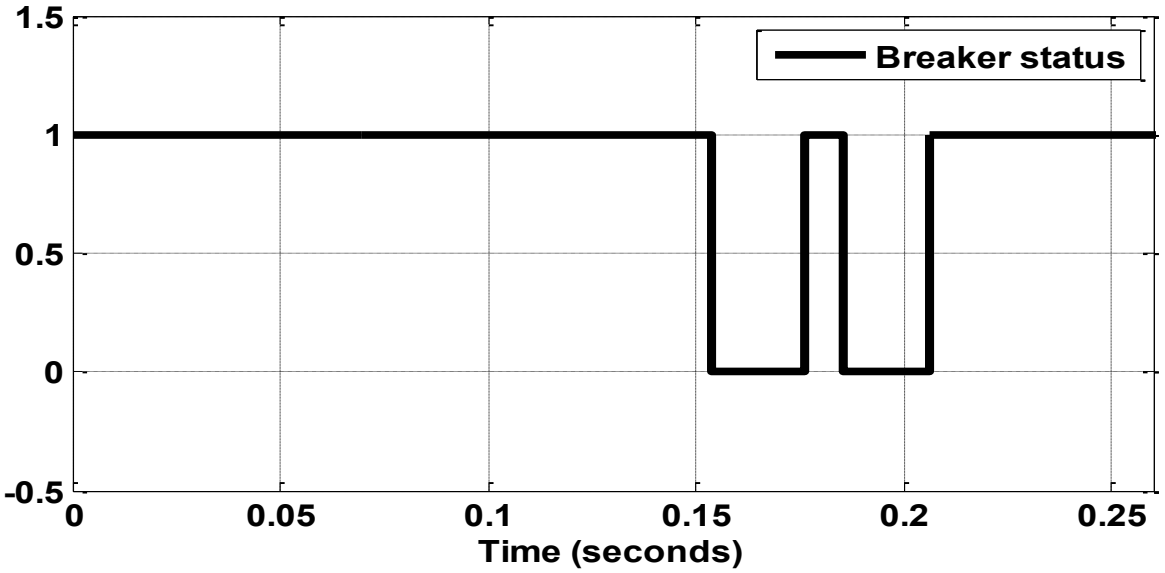

Fig. 3.15 Breaker status of load number 1 in case of overcurrent in the feeder (MATLAB/ SIMULINK results)

The simulation carried out on eMEGASim® OP5600 OPAL-RT real-time simulator regarding the protection of three-phase feeder of area 1 against overcurrent by local controller placed at DT_1, are presented below:

The plot of phase currents (RMS value) vs. the time of DT_1 secondary winding has been shown in Fig. 3.16. It is observed from Fig. 3.16 that current in phase A of DT_1 secondary winding exceeded by 16% from its rated value of 3478 amperes at time t=0.17sec. Since phase current exceeded by more than 10%, it was considered a case of overcurrent in phase A, by the local controller. Local controller checked smart meter readings of all the loads connected in phase A of area 1. It was observed that load number 1 demand exceeded its sanctioned value and power factor of load number 1 was 0.846, which was slightly less than 0.85. A smart meter reading of all other loads connected to phase A was observed to be less than their sanctioned demand value, and their power factor were also more than 0.85. Therefore, the local controller placed at DT_1 considered power drawn by load number 1 as the cause of overcurrent, and disconnected it at time t=0.185sec, as shown in Fig. 3.16. It is observed from Fig. 3.16 that phase A current of DT_1 secondary winding is brought down to less than 1.1 times of its rated value at time t=0.195sec due to disconnection of load number 1 at time t=0.185sec. Therefore, load number 1 was reconnected at time t=0.196sec. It is observed from Fig. 3.16 that the reconnection of load number 1 again exceeded phase A current by 12% at time t=0.21sec., as the extra load connected to load number 1 again became ON. Sensing overcurrent, local controller checked reading of all smart meters connected to phase A. It was observed that load number 1 was still drawing more than sanctioned demand. Hence, the local controller disconnected it at time t=0.23sec. Disconnection of load number 1 brought down phase A current to less than 1.1 times DT_1 secondary winding rated current value at time t=0.23sec, as observed from Fig. 3.16. Therefore load number 1 was reconnected by the local controller at time t=0.231sec. It is again observed that the reconnection of load number 1 exceeded phase A current by 12% at time t=0.239sec., as the extra load connected to load number 1 again became ON. Sensing overcurrent, local controller checked reading of all smart meters connected to

phase A. It was observed that load number 1 was still drawing more than sanctioned demand. Hence, the local controller disconnected it at time t=0.25sec. Disconnection of load number 1 brought down phase A current to less than 1.1 times DT_1 secondary winding rated current value at time t=0.26sec, as observed from Fig. 3.16. Therefore load number 1 was reconnected by the local controller at time t=0.262sec.

Breaker status of load number 1 has been shown in Fig. 3.17. It is observed from Fig. 3.17 that breaker status of load number 1 is 0 (i.e. OFF status) for the period 0.185sec to 0.195sec, 0.21sec to 0.23sec and 0.24sec to 0.26sec, whereas, its status is 1 (i.e. ON status) for the remaining period. This is because load number 1 was disconnected by the local controller at time t=0.185sec, switched ON at time t=0.195sec, again disconnected at time t=0.21sec, and again switched ON at time t=0.23sec, again disconnected at time t=0.24sec, and again switched ON at time t=0.26sec.

It is further observed from Fig. 3.16 that phase C current of DT_1 secondary winding exceeded its rated value by 19.5% at time t=0.225sec. Local controller checked all smart meter readings connected to phase C. None of the smart meter reading was found to exceed its sanctioned demand value/power factor becoming less than 0.85. Hence, further investigations were carried out regarding power theft in phase C. Simulation results regarding power theft detection have been presented in Section 3.3.4.

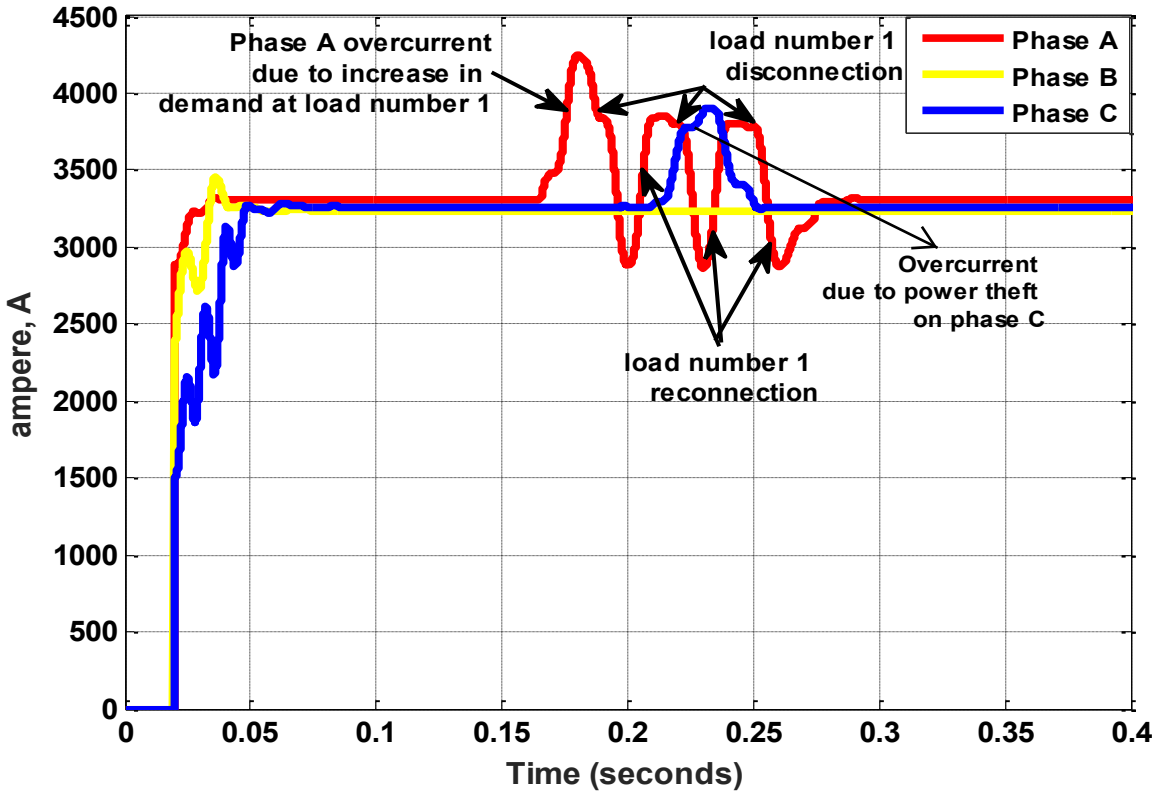

Fig. 3.16 Phase currents (RMS value) of DT_1 secondary winding in case of overcurrent in the feeder (OPAL-RT results)

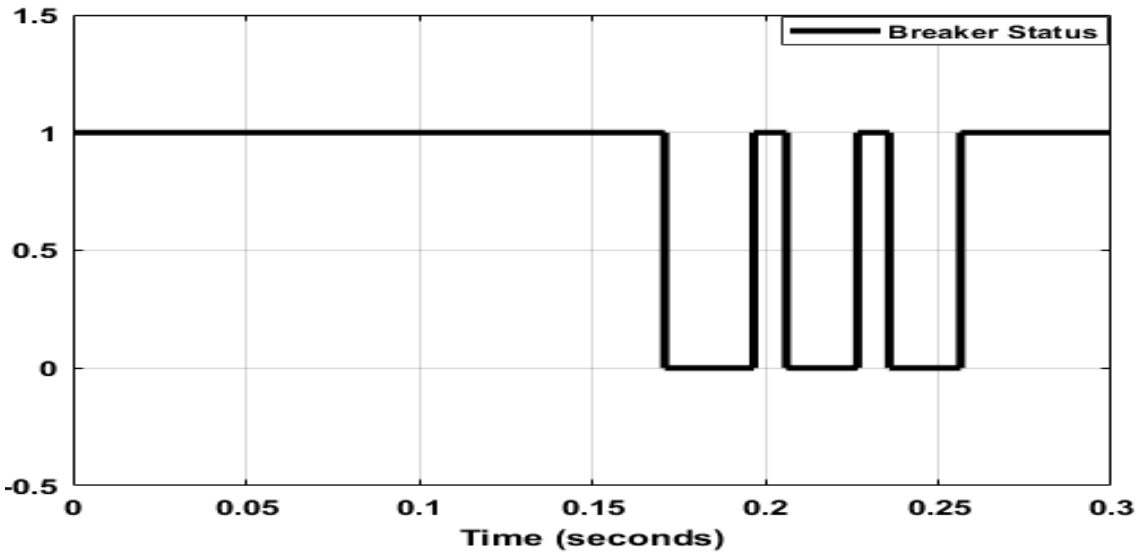

Fig. 3.17 Breaker status of load number 1 in case of overcurrent in the feeder (OPAL-RT results)

It is observed from Fig. 3.13, Fig. 3.15, Fig. 3.16, and Fig. 3.17 that simulation results obtained on developed MATLAB/ SIMULINK model closely match with results obtained on eMEGASim® OP5600 OPAL-RT real-time simulator.

3.3.4 Theft detection

An illegal real and reactive power load of 150kW and 80kVAr respectively was connected in phase C of area 1 near DT_1 secondary winding at time t=0.21sec and was removed at time t=0.23sec. This resulted in phase C current to exceed by 19.4% from its rated value of 3478 amperes at time t=0.228sec, as shown in Fig. 3.13 (MATLAB/ SIMULINK results). eMEGASim® OP5600 OPAL-RT results shown in Fig. 3.16 shows phase C current to exceed by 19.5% from its rated value at time t=0.225sec. Since none of the smart meter reading was showing power drawn by different loads more than their sanctioned demand value and power factor reading of all smart meters were more than 0.85, further investigations were carried out regarding theft by the local controller at DT_1 using the algorithm presented in Section 3.2.3. Local controller observed DT_1 secondary current in phase A, phase B and phase C as 3208.21A, 3390A and 3899.5A, respectively, whereas, the magnitude of the vector sum of currents drawn by all legal loads connected to phase A, phase B and phase C were found to be 3306.78A, 3287.40A and 3265.1A respectively. This resulted in percentage value of $[I_{s,\,A} - |\sum \bar{I}_{ph,\,A}|] / [|\sum \bar{I}_{ph,\,A}|]$, $[I_{s,\,B} - |\sum \bar{I}_{ph,\,B}|] / [|\sum \bar{I}_{ph,\,B}|]$ and $[I_{s,\,C} - |\sum \bar{I}_{ph,\,C}|] / [|\sum \bar{I}_{ph,\,C}|]$ as 3%, 3.12% and 19.4% for phase A, phase B and Phase C, respectively. The vector sum of currents drawn by all legal loads was calculated by the local controller using current and power factor readings of smart meters and voltage drop in different sections of phase A, phase B and phase C of the feeder with respect to a common reference. Since phase C current of the secondary winding of feeder was exceeding by 19.4% the magnitude of the vector sum of current drawn by all legal loads connected to phase C of the feeder of area 1, local controller notified theft notice to the system administrator. MATLAB command window shown in Fig. 3.18 shows theft notification to the system administrator at time t=0.21sec.

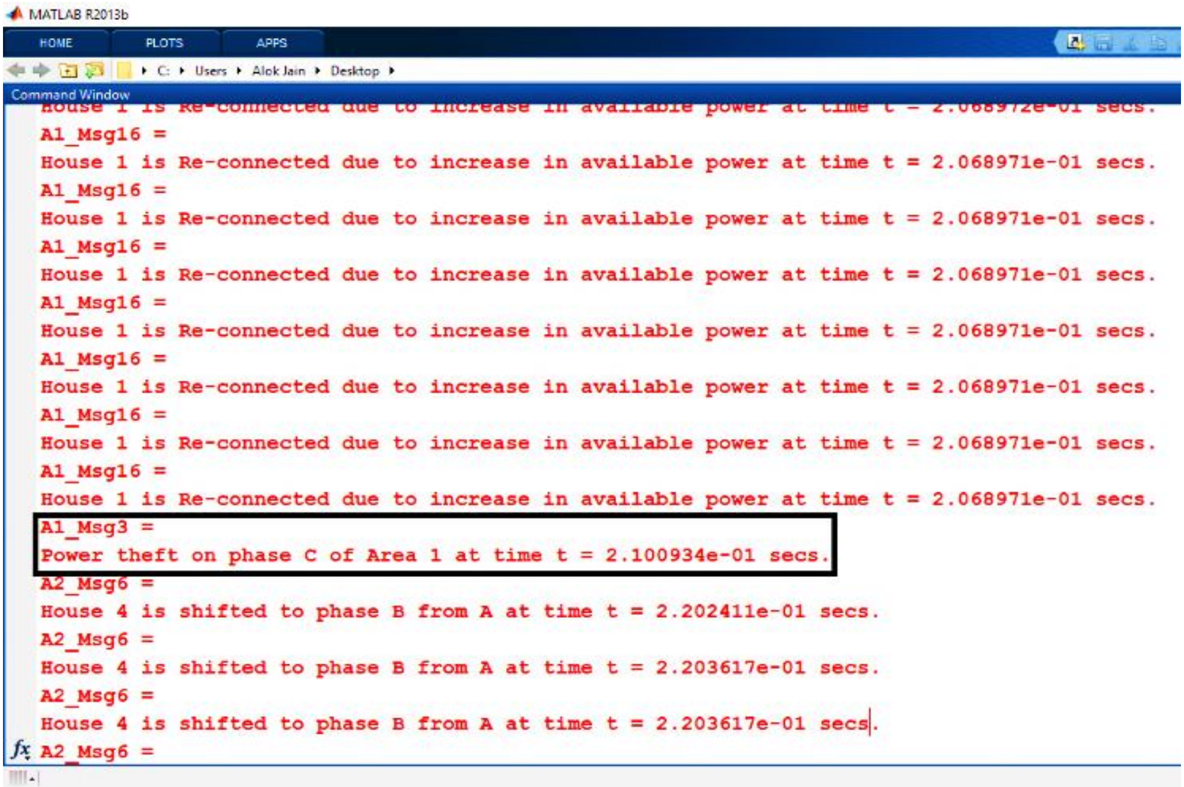

Fig. 3.18 MATLAB command window is showing notification of theft at time t=0.21sec.

3.3.5 Simultaneous control of events

MATLAB/SIMULINK results of Simultaneous control of load balancing, overcurrent protection of feeder, and theft detection of area 2 by the local controller based on the flowchart presented in Section 3.2.4 are presented below:

The plot of DT_2 secondary phase currents (root mean square (RMS) value) vs. time has been shown in Fig. 3.19, whereas, the plot of percentage phase unbalance factor (PUF) vs. time has been shown in Fig. 3.20. It is observed from Fig. 3.20 that the PUF was less than 10% up to 0.16sec, thus requiring no action regarding load balancing. Load number 8 and 20 of phase B were switched off at time t=0.16sec. This caused the drop in phase B current, as shown in Fig. 3.19. It is observed from Fig. 3.20 that PUF becomes more than 10% due to disconnection of load number 8 and 20. Based on the load balancing algorithm presented

in Section 3.2.1, real power, as well as reactive power demand of load number 4 of phase A, were shifted to phase B at time t=0.25sec as shown in Fig. 3.19. This brought down the phase unbalance factor to less than 10% value at time t=0.36sec, as observed from Fig. 3.20. Therefore, load number 8 and 20 were reconnected at time t=0.36sec, as shown in Fig. 3.19. Reconnection of load number 8 and 20 of phase B caused the rise in phase B current, which resulted in PUF of more than 10% again, as observed from Fig. 3.20 which resulted in phase unbalance factor of more than 10% again, as seen from Fig. 3.20. Based on the load balancing process presented in Section 3.2.1, real power, as well as reactive power demand of load number 11 of phase B, were shifted to phase A at time t=0.41sec as shown in Fig. 3.19. This brought down the phase unbalance factor to less than 10% as observed from Fig. 3.20.

An extra load consisting of real power demand and reactive power demand of 150kW and 150kVAr, respectively to load number 2 of phase B in area 2 was connected at time t=0.36sec. Based on the overcurrent protection of the feeder algorithm presented in Section 3.2.2, it is observed from Fig. 3.19 that the current in phase B of DT_2 secondary winding exceeded by 13% from its rated value 3478 amperes at time t=0.37sec. Since phase current exceeded by more than 10%, it was considered a case of overcurrent in phase B, by the local controller. Local controller compares magnitude of DT secondary current in phase B with magnitude of vector sum of all load currents in phase B. Since, the difference was less than 10%, overcurrent was not due to theft. Local controller checked smart meter readings of all the loads connected in phase B of area 2. It was observed that load number 2 demand exceeded its sanctioned value and power factor of load number 2 was 0.84, which was slightly less than 0.85. Smart meter reading of all other loads connected to phase B was observed to be less than their sanctioned demand value, and their power factor were also more than 0.85. Therefore, the local controller placed at DT_2 considered power drawn by

load number 2 as the cause of overcurrent, and disconnected it at time t=0.39sec, as shown in Fig. 3.19. It is observed from Fig. 3.19 that phase B current of DT_2 secondary winding is brought down to less than 1.1 times of its rated value at time t=0.39sec due to disconnection of load number 2 at time t=0.39sec. Therefore, load number 2 was reconnected at time t=0.43sec. Now, PUF is again checked and is found that PUF is less than 10%.

An illegal real and reactive power demand of 250kW and 100kVAr, respectively was connected in phase B at time t=0.61sec and was removed at time t=0.65sec. Overcurrent protection of feeder algorithm detected an overcurrent of 14%. Based on the power theft algorithm in Section 3.2.3, local controller observed DT_2 secondary current in phase B as 3990 amperes whereas, the magnitude of the vector sum of currents drawn by all legal loads connected to phase B was calculated as 3265.1 amperes. The vector sum of currents drawn by all legal loads was calculated by the local controller using current and power factor readings of smart meters and voltage drop in different sections of phase B of the feeder with respect to a common reference. Since phase B current of the secondary winding of transformer was exceeding by 18% the magnitude of the vector sum of current drawn by all legal loads connected to phase B of the feeder of area 2, local controller notified theft notice to the system administrator. The theft was removed at time t=0.65sec and it is observed from Fig. 3.19 that overcurrent caused due to theft is controlled.

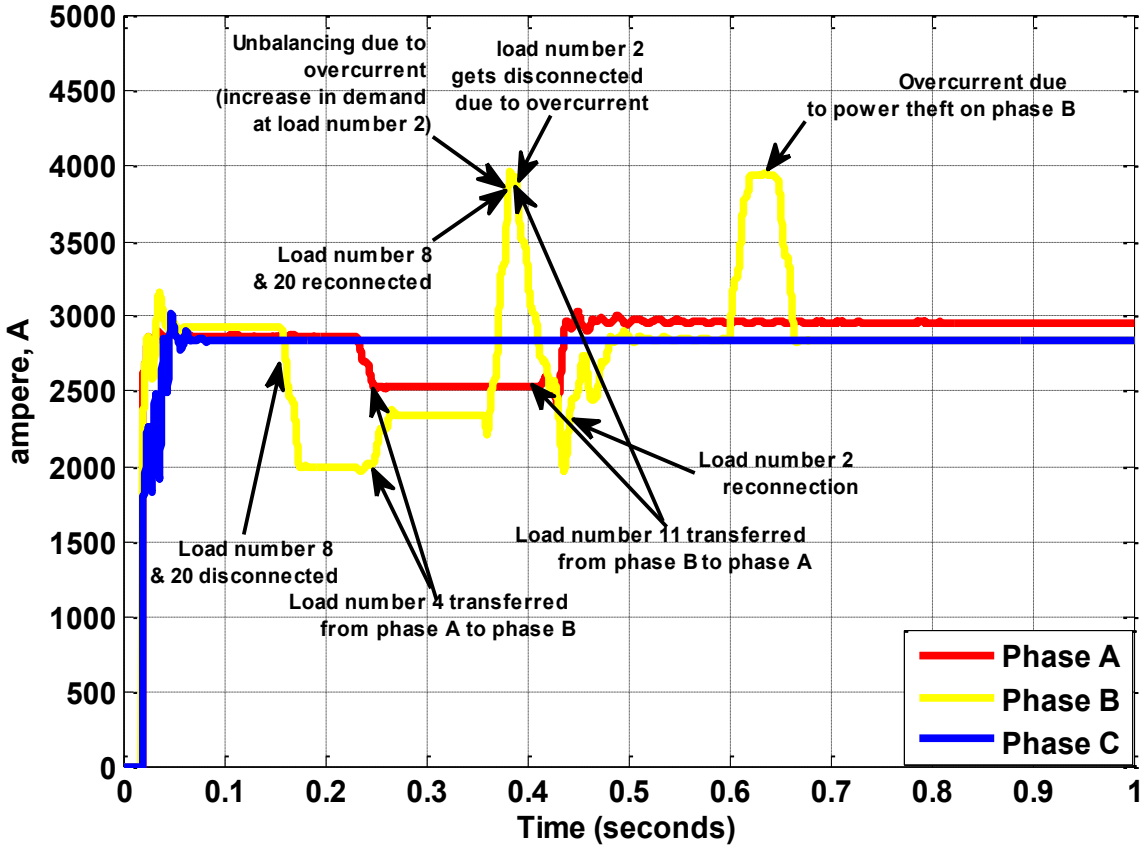

Fig. 3.19 Simultaneous control of load balancing, overcurrent protection of feeder, and theft detection (MATLAB /SIMULINK results)

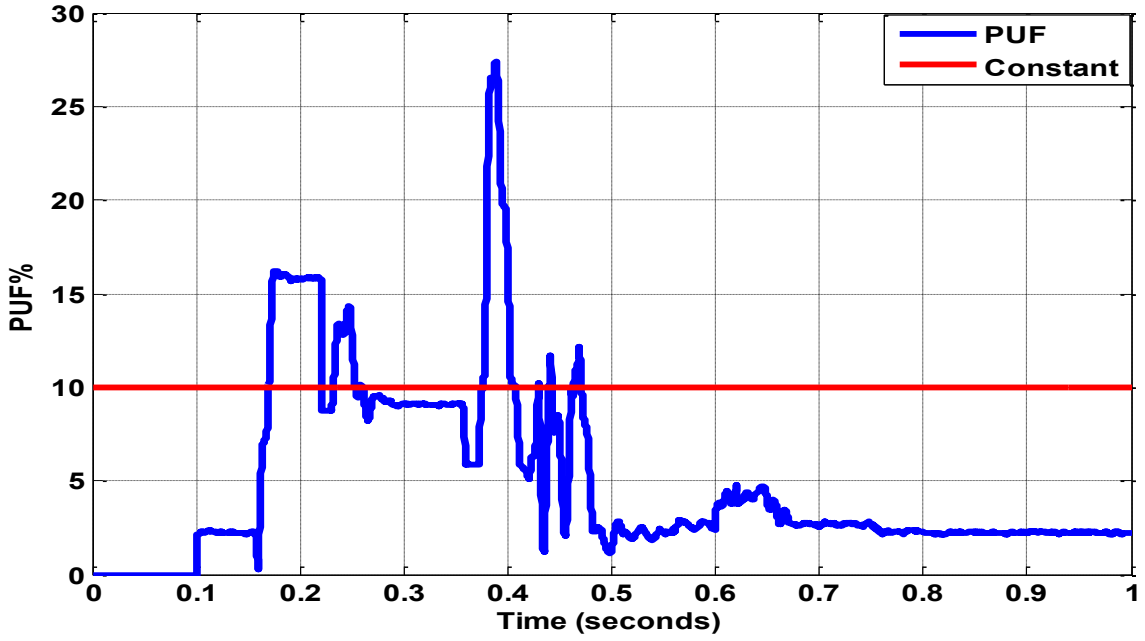

Fig. 3.20 Percentage phase unbalance factor (MATLAB /SIMULINK results)

OPAL-RT results of Simultaneous control of load balancing, overcurrent protection of feeder, and theft detection of area 2 by the local controller are presented below:

The plot of DT_2 secondary phase currents (root mean square (RMS) value) vs. time has been shown in Fig. 3.21, whereas, the plot of percentage phase unbalance factor (PUF) vs. time has been shown in Fig. 3.22. It is observed from Fig. 3.21 that the PUF was less than 10% up to 0.158sec, thus requiring no action regarding load balancing. Load number 8 and 20 of phase B were switched off at time t=0.158sec. This caused the drop in phase B current, as shown in Fig. 3.21. It is observed from Fig. 3.22 that PUF becomes more than 10% due to disconnection of load number 8 and 20. Based on the load balancing algorithm presented in Section 3.2.1, real power, as well as reactive power demand of load number 4 of phase A, were shifted to phase B at time t=0.24sec as shown in Fig. 3.21. This brought down the phase unbalance factor to less than 10% value at time t=0.358sec, as observed from Fig. 3.22. Therefore, load number 8 and 20 were reconnected at time t=0.358sec, as shown in Fig. 3.21. Reconnection of load number 8 and 20 of phase B caused the rise in phase B current, which resulted in PUF of more than 10% again, as observed from Fig. 3.21 which resulted in phase unbalance factor of more than 10% again, as seen from Fig. 3.22. Based on the load balancing process presented in Section 3.2.1, real power, as well as reactive power demand of load number 11 of phase B, were shifted to phase A at time t=0.408sec as shown in Fig. 3.21. This brought down the phase unbalance factor to less than 10% as observed from Fig. 3.22.

An extra load consisting of real power demand and reactive power demand of 150kW and 150kVAr, respectively was connected to load number 2 of phase B in area 2 at time t=0.358sec. Based on the overcurrent protection of the feeder algorithm presented in Section 3.2.2, it is observed from Fig. 3.21 that the current in phase B of DT_2 secondary winding exceeded by 13% from its rated value 3478 amperes at time t=0.368sec. Since

phase current exceeded by more than 10%, it was considered a case of overcurrent in phase B, by the local controller. Local controller compares DT_2 secondary current magnitude with magnitude of vector sum of all load currents in phase B. Since, the difference was less than 10%, it was not a case of theft. Local controller checked smart meter readings of all the loads connected in phase B of area 2. It was observed that load number 2 demand exceeded its sanctioned value and power factor of load number 2 was 0.84, which was slightly less than 0.85. Smart meter reading of all other loads connected to phase B was observed to be less than their sanctioned demand value, and their power factor were also more than 0.85. Therefore, the local controller placed at DT_2 considered power drawn by load number 2 as the cause of overcurrent, and disconnected it at time t=0.39sec, as shown in Fig. 3.21. It is observed from Fig. 3.21 that phase B current of DT_2 secondary winding is brought down to less than 1.1 times of its rated value at time t=0.39sec due to disconnection of load number 2 at time t=0.39sec. Therefore, load number 2 was reconnected at time t=0.42sec. Now, PUF is again checked and is found that PUF is less than 10%.

An illegal load consisting of real power demand of 250kW and reactive power demand of 100kVAr was connected in phase B at time t=0.61sec and was removed at time t=0.65sec. Overcurrent protection of feeder algorithm detected an overcurrent of 14%. Based on the power theft algorithm in Section 3.2.3, local controller observed DT_2 secondary current in phase B as 3990 amperes whereas, the magnitude of the vector sum of currents drawn by all legal loads connected to phase B was calculated as 3265.1 amperes. The vector sum of currents drawn by all legal loads was calculated by the local controller using current and power factor readings of smart meters and voltage drop in different sections of phase B of the feeder with respect a common reference. Since phase B current of the secondary winding of transformer was exceeding by 18% the magnitude of the vector sum of current drawn by all legal loads connected to phase B of the feeder of area 2, local

controller notified theft notice to the system administrator. The theft was removed at time t=0.65sec and overcurrent due to theft was controlled.

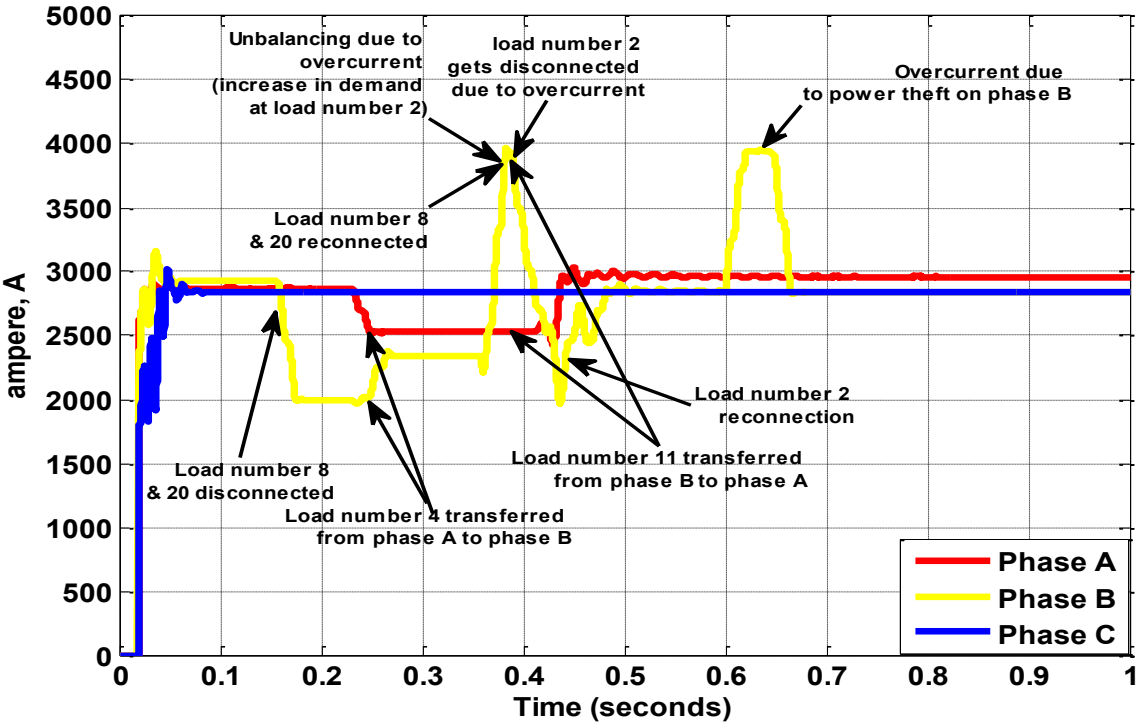

Fig. 3.21 Simultaneous control of load balancing, overcurrent protection of feeder, and theft detection (OPAL-RT results)

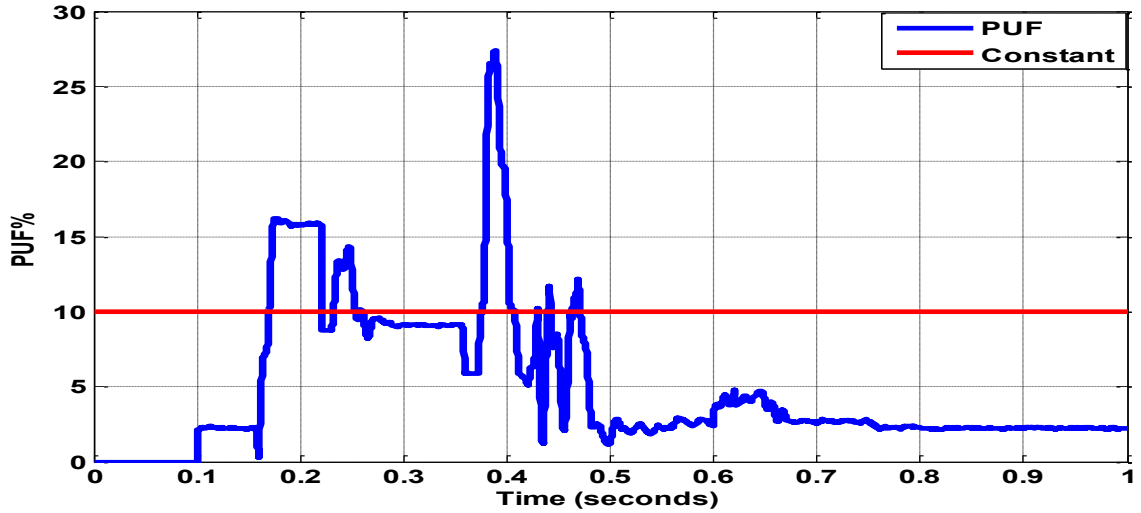

Fig. 3.22 Percentage phase unbalance factor (OPAL-RT results)

It is observed from Fig. 3.19, Fig. 3.20, Fig. 3.21, and Fig. 3.22 that simulation results obtained on developed MATLAB/ SIMULINK model closely match with results obtained on eMEGASim® OP5600 OPAL-RT real-time simulator.

3.4 SUMMARY

A smart distribution system consisting of two level control architecture has been proposed. Master controller proposed to be installed at substation feeding distribution network through distribution transformers continuously checks available power at the substation and instructs local controller placed at distribution transformers to disconnect/reconnect loads based on power available at the substation from the grid. Apart from load shedding/load reconnection based on available power, local controllers address the problems of load balancing, protection of feeder against overcurrent, and theft detection based on smart meter readings. The bidirectional flow of information takes place between the master controller and local controllers, and between the local controller and smart meters, through Information and Communications Technology (ICT). Case studies have been performed on a test system comprising of two identical areas with each area consisting of 21 loads. Simulations carried out on developed MATLAB/ SIMULINK model of the test system were validated on an eMEGASim® OP5600 OPAL-RT real-time simulator. Present work considers notification to the system administrator in case of power theft detection.